ELSEVIER

PII: S0032-3861(97)00605-8

Polymer Vol. 39 No. 17, pp. 4065–4074, 1998
© 1998 Elsevier Science Ltd
Printed in Great Britain. All rights reserved
0032-3861/98/\$19.00+0.00

Effect of copolymer composition in vinyl silane modified polyvinylimidazole on copper corrosion protection at elevated temperature

Hyuncheol Kim and Jyongsik Jang*
Department of Chemical Technology, Seoul National University, San 56-1, Shinlimdong Kwanakgu, Seoul, South Korea
(Received 27 January 1997; revised 12 June 1997; accepted 11 July 1997)

The copolymer of vinyl imidazole (VI) and vinyl trimethoxy silane (VTS), was synthesized in benzene at 68°C as a novel corrosion inhibitor for copper. The effect of the copolymer composition on copper corrosion protection at elevated temperatures was investigated by Fourier transform infrared reflection, absorption spectroscopy (FTIR-RAS) and scanning electron microscopy (SEM). In addition, an adhesion test was performed to characterize the interface between copper and the polymer film after heat treatment. Corrosion protection capabilities of the copolymer at 360°C in air was improved via increasing the mol ratio of VTS in the feed, due to the improved thermal stability and the reactivity of the copolymer with copper. © 1998 Elsevier Science Ltd. All rights reserved.

(Keywords: corrosion inhibitor for copper; copolymer composition; silane modified polyvinylimidazole)

INTRODUCTION

Protective organic coatings on copper surfaces are necessary to protect its surface in corrosive environments. Imidazole and its derivatives have been known as effective corrosion inhibitors for copper and its alloy[1–16]. It was reported that imidazole derivatives inhibit the adsorption of air oxygen onto copper surfaces through a complex formation between the surface and nitrogen in imidazole rings[17–23]. Eng *et al.* reported that polyvinylimidazole (PVI) suppressed the oxidation of copper surfaces above 200°C in air[13–16]. Jang *et al.* introduced a silane coupling agent (γ-MPS) into PVI to improve the adhesion between the polymer film and copper surfaces, and to suppress the corrosion of such surfaces at elevated temperatures[24,25]. However, thermal degradation of the polymer film might lead to the cuprous oxide formation on copper surfaces at elevated temperatures. On the other hand, Kim *et al.* synthesized the various silane modified PVI(1)s, whose mole fractions are 1:1, with the different siloxane linkages per weight, and tested their corrosion protection capability at elevated temperatures[26]. Corrosion protection capability depended on the thermal stability of the silane modified PVI(1)s, which was at the mercy of a number of the siloxane linkages per weight. Poly(VI-co-VTS) showed the highest corrosion protection capability at elevated temperatures, due to its higher thermal stability.

In this paper, poly(VI-co-VTS), with high thermal stability was synthesized from VI and VTS by changing the mole ratios of the two monomers in the feed. The corrosion protection of the copolymers for copper surface at elevated temperatures was investigated with FTIR-RAS and SEM. In addition, the changes of the corrosion behaviour and the corrosion mechanisms via changing mole fraction of VTS were studied with the aid of adhesion tests.

* To whom all correspondence should be addressed

EXPERIMENTAL

VI and VTS (Aldrich Chemical Co.) were distilled *in vacuo* to yield pure and colourless liquids. AIBN (Wako Pure Chemical Industries Ltd.) was dissolved in warm methanol (35°C), recrystallized in an ice bath, and then dried in a vacuum oven at room temperature for 2 days.

Poly(VI-co-VTS)s were synthesized by free radical copolymerization using AIBN as an initiator. VI and VTS were copolymerized in benzene at 68°C by stirring in an argon atmosphere. The total monomer concentration was 2 M, and the initiator concentration was fixed at 2×10^{-3} M. The mole ratios of VI to VTS in the feed were 85:15, 70:30 and 50:50, but the mole ratios of VI to VTS in the copolymer were 90.51:9.49, 81.56:28.44 and 67.37:22.63, respectively. The copolymerization scheme of VI and VTS is shown in *Figure 1*.

Copper plates (1.2 cm × 5.0 cm × 0.3 cm) were mechanically polished with a No. 5 chrome oxide, washed with *n*-hexane and acetone in an ultrasonic bath, rinsed with 1% HCl/distilled water solution, distilled water and acetone, and then dried with a stream of nitrogen gas. Copolymer solution was cast onto copper plates with a microsyringe and the samples were dried at 60°C for 12 h in air before corrosion tests to remove the residual solvent in the copolymer film. Polymer-coated copper plates were heated at 360°C for 15 min in air. Film thickness was calculated, based on the concentration of the copolymer solution, copolymer density and the area of the copper surface. In this study 2 μm thick films were used.

Adhesion test (ASTM D3359-83 Tape test) was performed to investigate the adhesion strength between copper surface and the thermally degraded copolymer using an adhesive tape. This tape test is used to assess the adhesion of coated polymer on a metal surface, but it does not classify the coating materials of high adhesion strength.

Fourier transform infrared reflection and absorption spectroscopy (FTIR-RAS) was used to characterize the

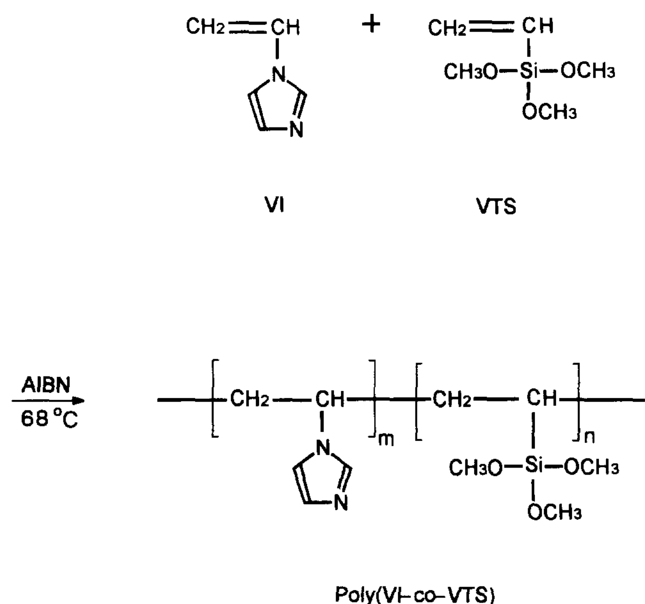

Figure 1 The copolymerization scheme of VI and VTS

polymers coated on copper surfaces, and to investigate the corrosion formation after heat treatment. In addition, polymer-coated copper surfaces after adhesion tests were studied. The spectrometer was continuously purged with dry nitrogen gas to remove water vapour and atmospheric CO_2. Absorbance spectra were obtained using Bomem MB-100 spectrometer at a resolution of 4 cm^{-1} and 100 scans were collected. Graseby Specac P/N 19650 monolayer/grazing angle accessory was used. The angle of incidence was 78° and a freshly polished copper coupon was used to obtain the reference spectrum.

The ^{1}H-NMR spectrum of poly(VI-co-VTS) dissolved in C_6D_6/Dimethyl-d_6 sulphoxide cosolvent was obtained by using a VXR-200 FT-NMR spectrophotometer. Tetramethyl silane was used as an internal standard material.

Scanning electron microscopy (SEM) was used to observe the corrosion formation of polymer-coated copper plates. The morphologies of polymer-coated copper surfaces before and after adhesion test were investigated. The instrument used in this experimental was Jeol JSM-35 and specimens were coated with a thin layer of gold to eliminate charging effects.

RESULTS AND DISCUSSION

FT-IR reflection and absorption spectra of PVI film and the copolymer films with the different mole fractions on copper plates are shown in *Figure 2*. Spectrum A demonstrates the characteristic peaks of VI at 3114 cm^{-1}, 1498 cm^{-1}, 1282 cm^{-1} and 1230 cm^{-1}. As VTS mole fractions in the copolymer increase, the characteristic peaks of VTS at 2945 cm^{-1}, 2842 cm^{-1} and 1154 cm^{-1} increase in intensities. The broad bands around 3421 cm^{-1} are assigned to the water peak. Silane modified PVI can contain residual water in the copolymer film due to the hydroscopic property of VI[14,27]. The details for the peak assignments of poly(VI-co-VTS) are represented in *Table 1*[14,28].

Figure 3 shows ^{1}H-NMR spectrum of the copolymer (VI/VTS = 7/3) dissolved in C_6D_6/Dimethyl-d_6 sulphoxide cosolvent. The peak at (**a**) is assigned to the proton of the copolymer backbone formed from a VI unit. Two peaks at (f) and (g) are associated with the protons of the copolymer

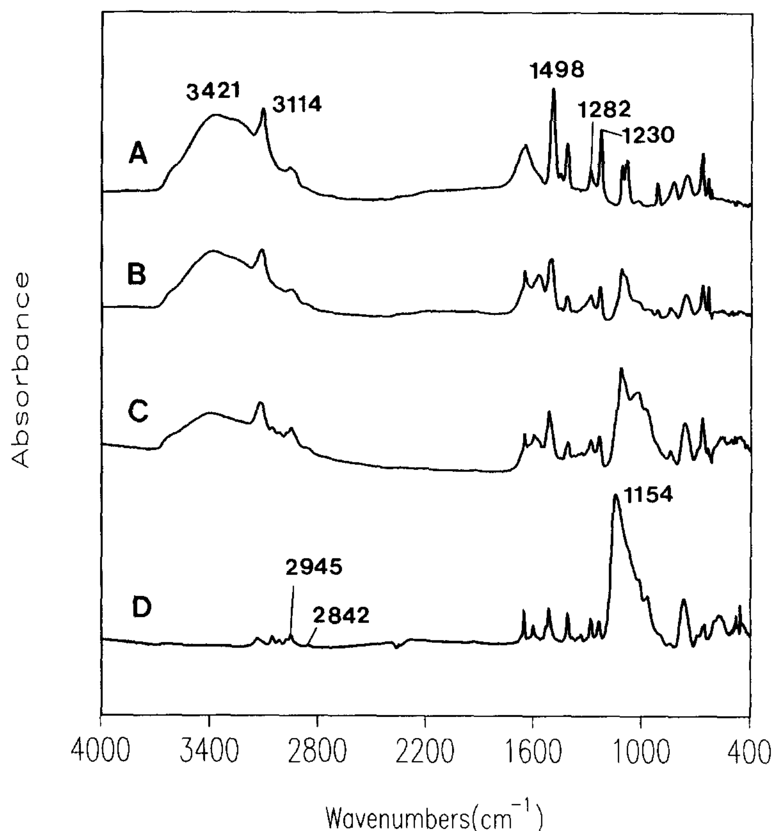

Figure 2 FT-JR reflection and absorption spectra of PVI film and the copolymer films with the different mol ratios on copper plates: (*A*) PVI, (*B*) VI/VTS = 85/15, (*C*) VI/VTS = 70/30, and (*D*) VI/VTS = 50/50

Table 1 Tentative infrared band assignments of poly(VI-co-VTS)

Band positions (cm^{-1})	Tentative assignments
3421	O-H from residual water
3114	C=C-H/N=C-H stretching
2945	CH_3 asymmetric stretching from Si-O-CH_3
2842	CH_3 symmetric stretching from Si-O-CH_3
1649	O-H deformation (water)/C=N stretching
1498	C=C/C=N stretching
1451	CH_2 bending (mostly) + ring stretching
1415	CH_2 bending (mostly) + ring stretching
1282	Ring vibrations
1230	Ring vibrations
1154	CH_3 rocking from Si-O-CH_3
1109	CH in-plane bending
1083	CH in-plane bending + Si-O-C asymmetric stretching
915	CH out-of-plane bending
816	CH out-of-plane bending + Si-O-C symmetric stretching
750	CH_2 bending
664	Ring torsion
638	C=C-H/N=C-H wagging

backbone from VTS unit. Especially, the proton peak from Si-C-H unit has a lower chemical shift than 1 due to the effect of the Si atom.

Polymer-coated copper plates were heated at elevated temperatures in air to test the corrosion protection capability of the copolymers with different mole fractions. *Figure 4* demonstrates FT-JR the reflection and absorption spectra of both PVI and the copolymer films with the different mole ratios on copper plates. All samples were heated at 360°C for 15 min in air. As the mole fraction of VTS in the copolymer increases, the polymer film coated on copper plates suffers less thermal degradation due to enhanced thermal stability through the siloxane network formation. The broad bands between 1700 cm^{-1} and 1500 cm^{-1} in spectrum A are attributed to the thermal oxidative degradation products of the polymer backbone and the imidazole ring[15]. Compared with spectrum A, spectra B–D demonstrate the broad bands in the 1300–900 cm^{-1} region, the peak at 810 cm^{-1}, and the peak at 470 cm^{-1}. These peaks are related to the Si-O-Si bond formation via the crosslinking reaction of the VTS unit in the copolymer. Their peak intensities increase as VTS fractions in the copolymer increase. The broad bands in the 1300–900 cm^{-1} region contain the stretching peaks from the Si-O-Si, Si-OH, and Si-O-Cu bonds[29,30]. The peak at 810 cm^{-1} is due to the Si-O-Si bending mode and the peak at 470 cm^{-1} is designated to the Si-O-Si rocking mode. These peaks suggest that VTS units in the copolymer are hydrolyzed and condensed to form the disiloxane linkages. The vaporization of residual water in the copolymer during heating may have helped the formation of a siloxane network[27,28]. To observe the extent of corrosion formation, the peaks in the 700–500 cm^{-1} region were investigated. Spectrum A and B show a CuO peak at 571 cm^{-1} and two Cu_2O peaks at 655 cm^{-1} and 611 cm^{-1}[31]. As the mole fraction of VTS in the copolymer increases, the intensity of CuO peak decreases. In spectrum C, no cupric oxide peak is observed at 571 cm^{-1}. The reduction of the CuO peak intensity is ascribed not only to the reduction of water hydrogen-bonding with the imidazole ring, but also to the role of VTS as a water scavenger[32], because water is consumed to hydrolyze VTS units in the copolymer film. Water in the polymer film has been known to accelerate CuO formation[33]. In addition, the total amount of copper oxide decreases as the mole ratio of VTS increases. No corrosion peak is observed in spectrum D.

Adhesion tests were performed to characterize the interface between copper surfaces and thermally degraded copolymer, using an adhesive tape. *Figure 5* demonstrates FT-JR reflection and absorption spectra of PVI film on copper plate before and after adhesion tests. After adhesion test, the peak intensities from the thermally oxidized products hardly decreased in spectrum B. but copper oxide peaks showed a remarkable reduction in intensities. Cupric oxide peaked at 561 cm^{-1}, disappeared—and small cuprous oxide peaks were observed at 655 cm^{-1} and 611 cm^{-1}. This can be confirmed by the subtracted spectrum C (spectrum A − spectrum B). Spectrum C shows strong copper oxide peaks, but hardly any polymer oxidation peaks. From these results it can be inferred that the part removed by the adhesion tape consists mainly of copper oxide and that a greater part of the thermally degraded PVI film still remains on the copper surface even after adhesion tests.

Figure 6 shows scanning electron micrographs of PVI film heated at 360°C for 15 min in air before and after

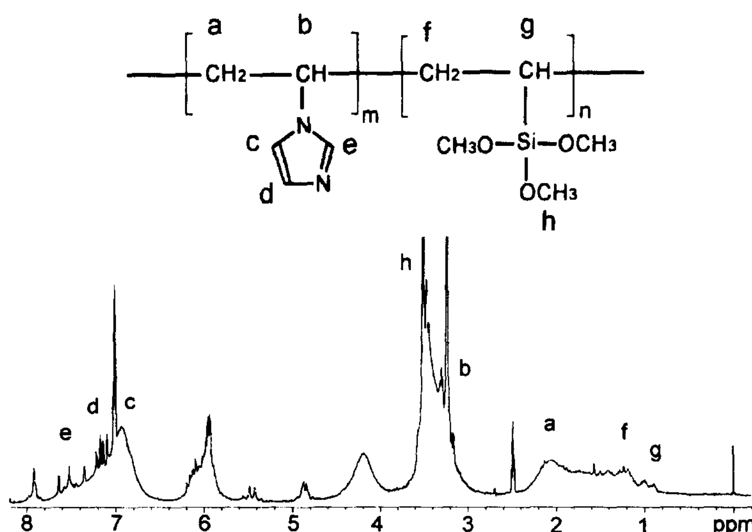

Figure 3 ^{1}H-NMR spectrum of the copolymer (VI/VTS = 7/3) dissolved in C_6D_6/Dimethyl-d_6 sulphoxide cosolvent

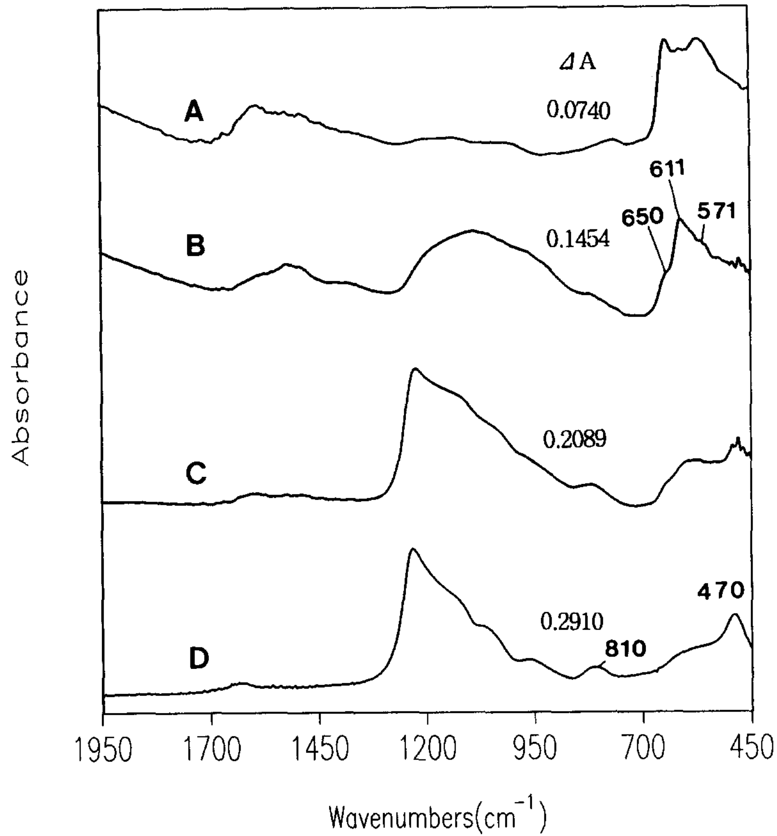

Figure 4 FT-JR reflection and absorption spectra of PVI film and the copolymer films with the different mol ratios on copper plates heated at 360°C for 15 min in air: (*A*) PVI, (*B*) VI/VTS = 85/15, (*C*) VI/VTS = 70/30, and (*D*) VI/VTS = 50/50

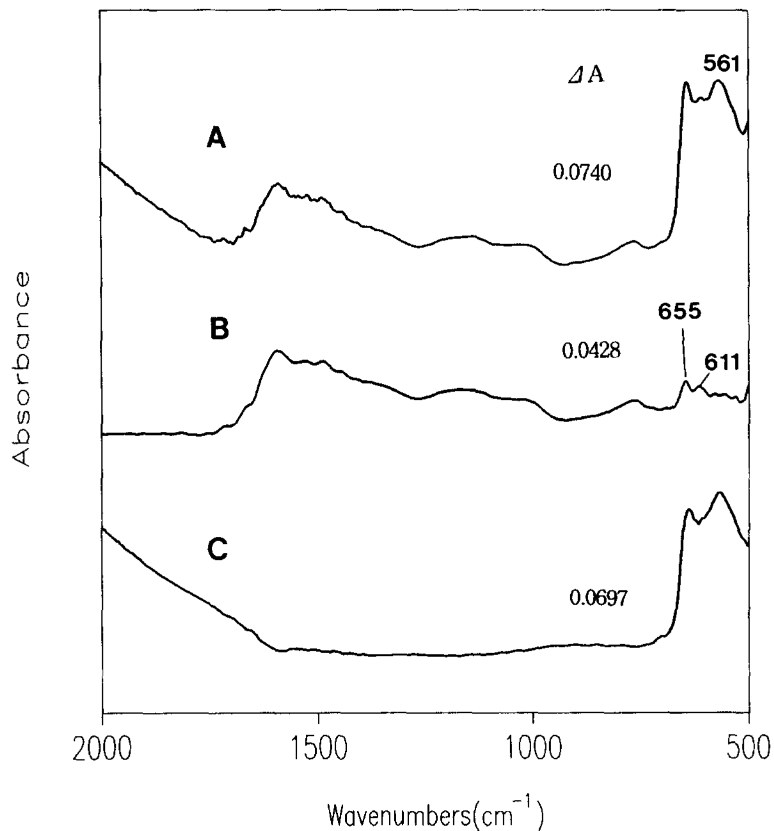

Figure 5 FT-JR reflection and absorption spectra of PVI film on copper plates heated at 360°C for 15 min in air: (*A*) PVI-coated copper surface before adhesion test, (*B*) copper surface after adhesion test, and (*C*) the part separated from copper surface (spectrum A – spectrum B)

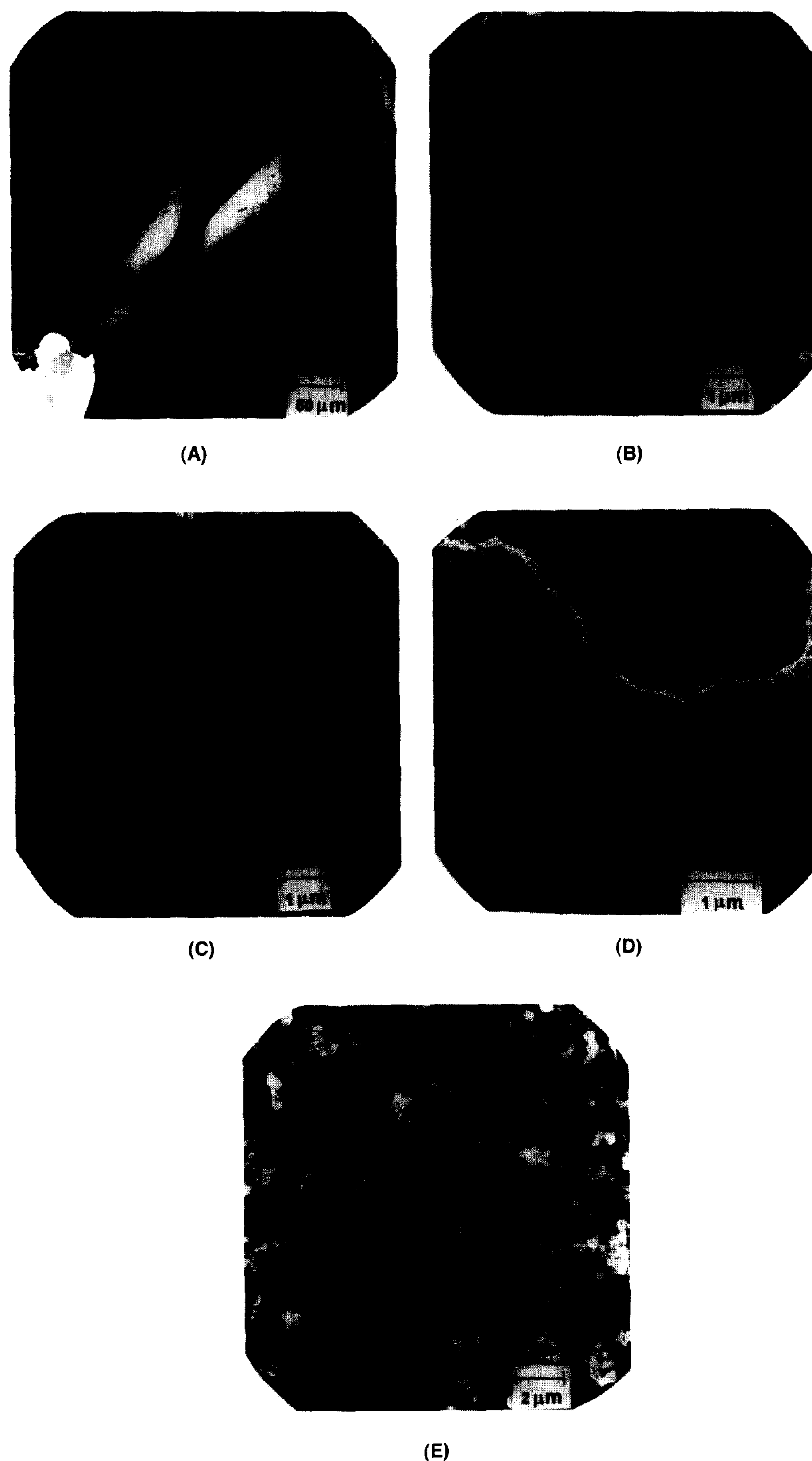

Figure 6 Scanning electron micrographs of PVI film on copper plate heated at 360°C for 15 min in air before and after adhesion test: (*A*) PVI-coated copper surface before adhesion test, (*B*) the enlarged view of **a** in (*A*), (*C*) the enlarged view of **b** in (*A*), (*D*) copper surface after adhesion test, and (*E*) the part separated from copper surface after adhesion test

adhesion test. PVI-coated copper surfaces before adhesion test is shown in *Figure 6*(*A*). The dark region (**b**), represents a part of the film which has flaked off during heat treatment. The bright region (**a**), indicates the surface of the thermally degraded PVI film, whose enlarged view is represented in *Figure 6*(*B*). The protruded crystals on the surface of PVI film are attributed to copper oxide crystals. This means that copper atoms of the copper surface diffused into the upper part of PVI film and reacted with air oxygen to form copper oxide crystals. *Figure 6*(*C*) shows the enlarged view of the dark region (**b**) in *Figure 6*(*A*). Small pits and pinholes are observed on the film surface. Considering that the size of the

pits is similar to that of copper oxide crystals in *Figure 6(B)*, they are thought to be formed when copper oxide crystals are separated from the oxidized PVI film. *Figure 6(D)* demonstrates a copper surface after adhesion tests. Two different regions exist in this photograph. A greater part of surface is composed of the porous structure with small pits and pinholes, and copper surface beneath the porous film is also observed. The porous structure indicates the thermally degraded PVI film. On the other hand, the existence of copper surface with copper oxide crystal, suggests that interfacial failure between copper and the porous PVI film occurred in part, and that copper oxide exists at the interface between copper and the porous film, as well as on the upper part of the porous film. *Figure 6(E)* shows the part removed from the porous film surface after an adhesion test, which is attached to the adhesion tape. Copper oxide crystals similar to those in *Figure 6(B)* were also observed. These SEM results are in accordance with the IR results in *Figure 5*.

IR spectra and SEM micrographs indicate that a good part of copper oxide is formed on the upper part of the porous film, but that some copper oxide, which is mainly composed of cuprous oxide, is present at the interface between copper and the porous film. Copper oxide formation on the porous film indicates the migration of copper through PVI film during thermal oxidation. This copper migration can be explained by matrix diffusion mechanism[34–38] and defect diffusion mechanism[38–40]. Matrix diffusion means the diffusion of copper from the copper surface into the bulk of the PVI film during heat treatment. Faupel *et al.* reported that copper can diffuse into a fully cured polyimide below the glass transition temperature[38]. Defect diffusion indicates the diffusion of copper through the film defects. The existence of pinholes in the porous structure [*Figure 6(D)*] indicates the chances of copper diffusion through film defects. Failure by adhesion test occurs at the interface between copper oxide and the porous film. Therefore, a great part of the porous film remains on the copper surface after adhesion tests. The schematic diagram of the oxidized PVI on copper plate is summarized in *Figure 7*. It consists of four different layers.

Figure 8 demonstrates FT-IR reflection and absorption spectra of the copolymer (VI/VTS = 85/15) film on copper plate before and after adhesion test. Compared with spectrum A, the peaks from the copolymer oxidation products are hardly observed in spectrum B. This indicates that most of the copolymer film coated on copper surfaces was removed from the surface. Some reduction in copper oxide peak intensity is also observed. This means that some of copper oxides were removed from the surface, and that the others still remain after adhesion tests. These facts can be confirmed by the subtracted spectrum C.

Scanning electron micrographs of the copolymer (VI/VTS = 85/15) film before and after adhesion tests are shown

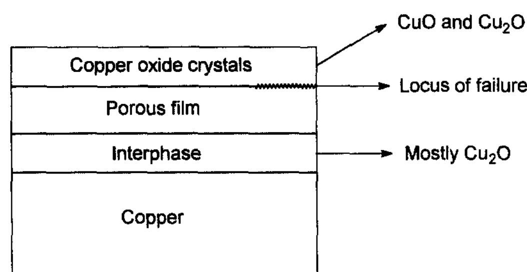

Figure 7 The schematic diagram of oxidized PVI on copper plate

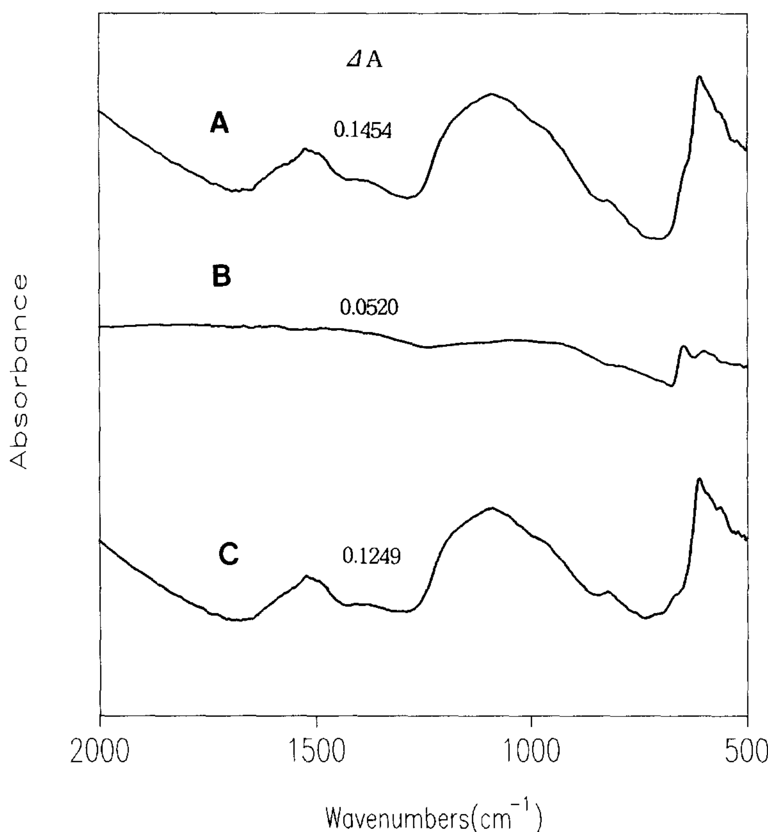

Figure 8 FT-JR reflection and absorption spectra of the copolymer (VI/VTS = 85/15) film on copper plate heated at 360°C for 15 min in air: (*A*) copolymer-coated copper surface before adhesion test, (*B*) copper surface after adhesion test, and (*C*) the part separated from copper surface (spectrum A – spectrum B)

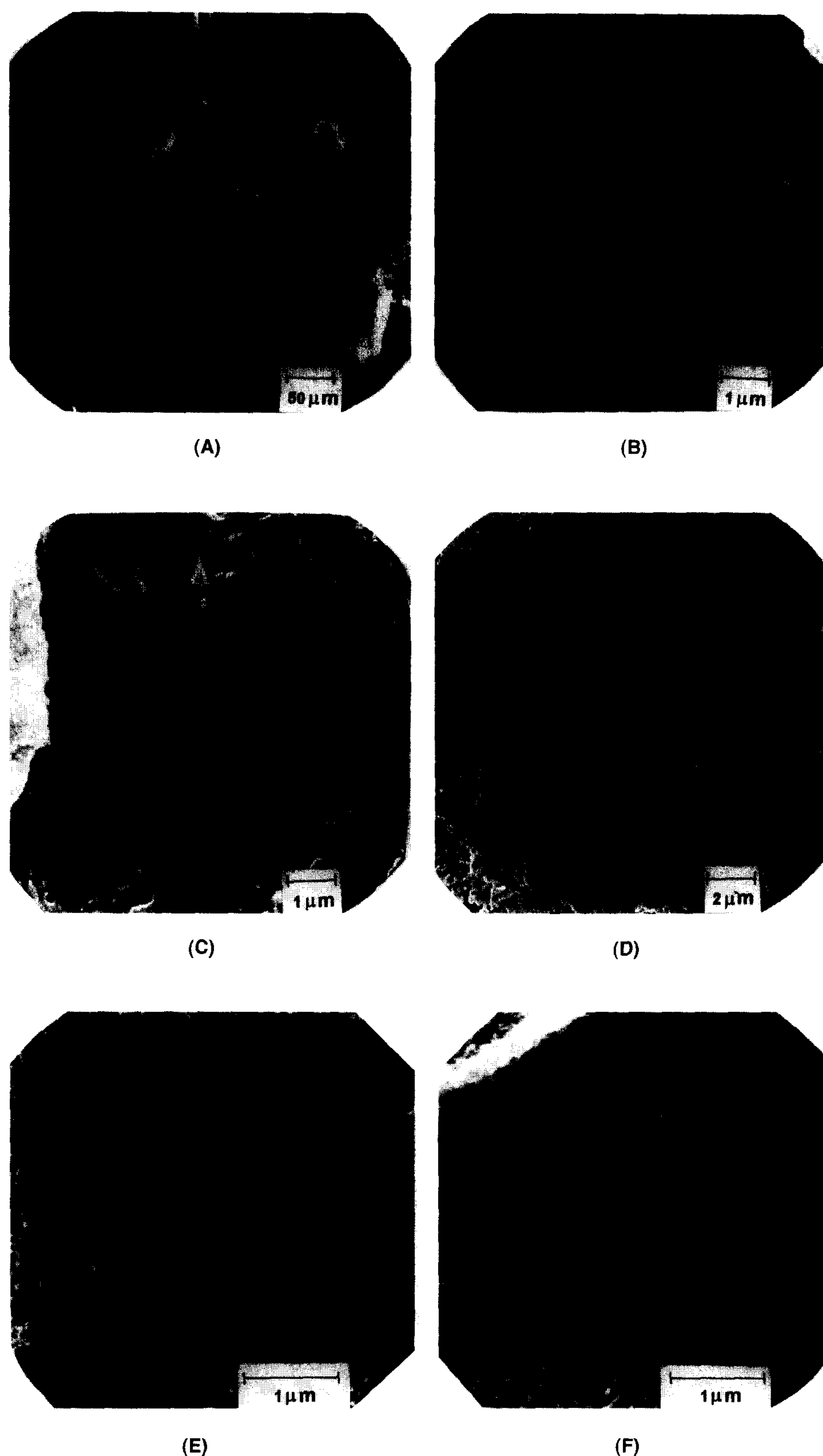

Figure 9 Scanning electron micrographs of the copolymer (VI/VTS = 85/15) film heated at 360°C in air for 15 min before and after adhesion test: (*A*) copolymer-coated copper surface before adhesion test, (*B*) the enlarged view of **a** in (*A*), (*C*) the enlarged view of **b** in (*A*), (*D*) copper surface after adhesion test, (*E*) the enlarged view of **a** in (*D*), and (*F*) the part separated from copper surface after adhesion test

in *Figure 9*. *Figure 9*(*A*) shows the copolymer-coated copper surface before adhesion test. It consists of two different regions. The bright part (**a**) represents the surface of the copolymer film, and its enlarged view is shown in *Figure 9*(*B*). Its surface contains some protruded parts, but distinct copper oxide crystals, as shown in *Figure 6*(*B*), are not seen. The dark part (**b**) in *Figure 9*(*A*) indicates the place where the copolymer film had flaked off due to the weakened copper-copolymer interface during heat treatment. Its enlarged view, as represented in *Figure 9*(*C*), shows the severely damaged copper surface. Copper surface after adhesion test is shown in *Figure 9*(*D*), which includes

two different regions: the unevenly etched copper surface and the remnants of the copolymer film. The one indicates that copper atoms in copper bulk diffuse into the copolymer film. The other (**a**) suggests that the interfacial adhesion between copper and the copolymer film is maintained to a certain degree in this region. Its enlarged view in *Figure 9(E)* shows copper oxide crystals. *Figure 9(F)* shows the polymer film part separated from the copper surface by an adhesive tape, and it is composed of two different regions. Its surface is well matched with copper surface after adhesion test [*Figure 9(D)*]. A rough surface (**a**) shows copper oxide crystals, and corresponds to the remnants of the copolymer film in *Figure 9(D)*. The outer smooth region (**b**) corresponds to the etched copper surface.

For the copolymer (VI/VTS = 85/15), most of the copper oxide crystals exist in the bulk of the copolymer film. This indicates that the introduction of VTS into PVI delays or inhibits the diffusion of copper from the surface into the bulk of the copolymer film. This is due to a strong chemical interaction of VTS with copper as well as the increased thermal stability of the copolymer. The formation of Si-O-Cu bond between the copper surface and the VTS unit in the copolymer suppresses the migration of copper from the surface into the bulk of the copolymer film. The existence of the Si-OH groups in the bulk of the film delays or inhibits the copper diffusion into the upper region of the film due to their strong chemical interaction with copper. The diffusion of transition metals into the polymer film becomes slower as the chemical interaction between metals and polymer becomes stronger[35,38]. In addition, the enhanced thermal stability of the copolymer can reduce the copper diffusion through the film defects due to the formation of the denser structure by the crosslinking of VTS unit. PVI film contains pinholes after heat treatment [*Figure 7(D)*], but these pinholes are no longer observed in the copolymer (VI/VTS = 85/15) film even if very fine defects might still exist in the copolymer film. The reduction in the number of pinholes decreases the copper diffusion into the copolymer film via these small holes[39,40]. The appearance of copper surface after adhesion tests shows an unevenly etched face. This inhomogeneity can be explained by the disproportion of Si-O-Cu bond formation on copper surface. The copper atoms bonded with VTS cannot diffuse into the bulk of film, but those not bonded with VTS can migrate from the surface into the bulk of the film. Accordingly, irregular pitches are formed on the copper surface. The schematic diagram of the copolymer (VI/VTS = 85/15) oxidized on copper plate is shown in *Figure 10*. Compared with the schematic diagram of PVI (*Figure 7*), it shows three different layers due to the inhibition of copper diffusion by VTS unit in the copolymer.

Figure 11 demonstrates FT-JR reflection and absorption spectra of the copolymer (VI/VTS = 70/30) film on copper plate heated at 360°C for 15 min in air. Spectrum B marginally shows the reductions in peak intensities in

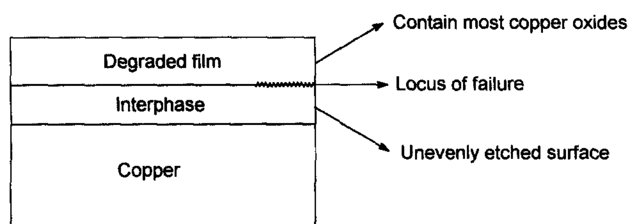

Figure 10 The schematic diagram of the copolymer (VI/VTS = 85/15) oxidized on copper plate

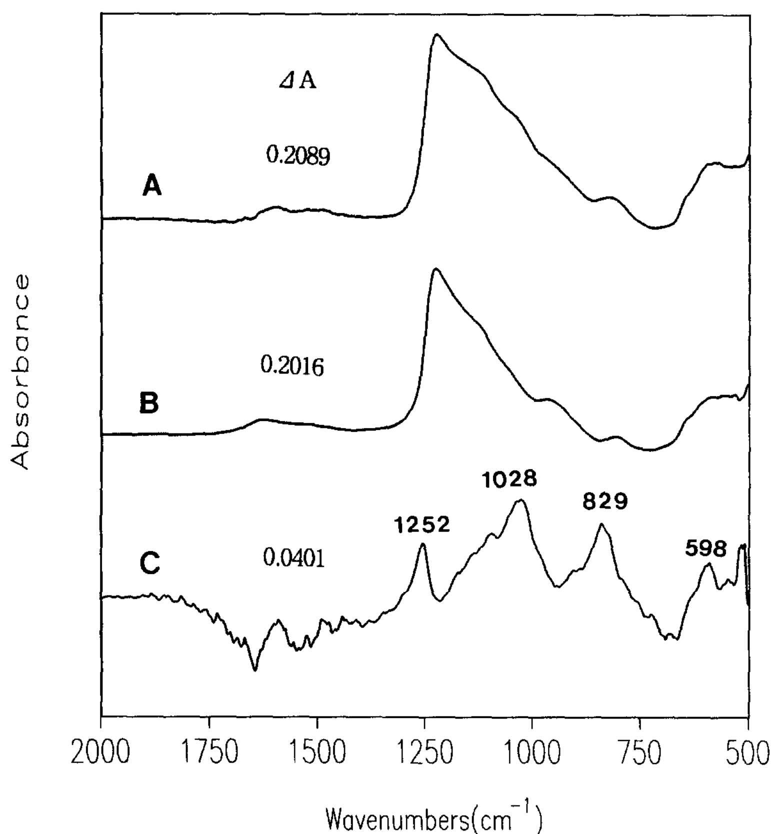

Figure 11 FT-JR reflection and absorption spectra of the copolymer (VI/VTS = 70/30) film on copper plate heated at 360°C for 15 min in air: (*A*) copolymer-coated copper surface before adhesion test, (*B*) copper surface after adhesion test, and (*C*) the part separated from copper surface (spectrum A – spectrum B)

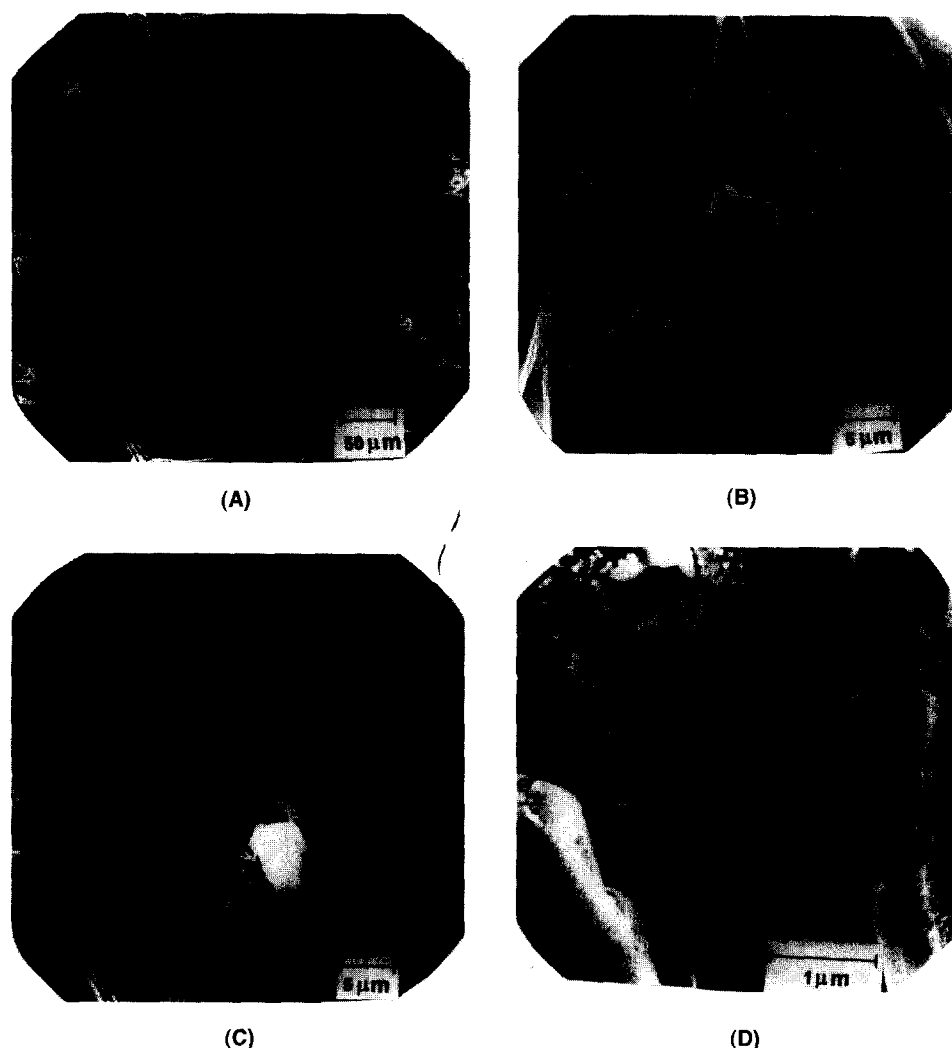

Figure 12 Scanning electron micrographs of the copolymer (VI/VTS = 70/30) film heated at 360°C for 15 min in air before and after adhesion test: (*A*) copolymer-coated copper surface before adhesion test, (*B*) the enlarged view of **a** in (*A*), (*C*) copper surface after adhesion test, and (*D*) the enlarged view of **a** in (*C*)

comparison with spectrum A. In the subtracted spectrum C, however, some small peaks from the disiloxane linkage are observed at $1252\ cm^{-1}$, $1028\ cm^{-1}$, and $829\ cm^{-1}$, and a copper oxide peak at $598\ cm^{-1}$. These peaks mean that only a small portion of the copolymer film, which contains some copper oxides, was removed from the copper surface, and that a great part of the copolymer film remains on copper surface after adhesion tests. Consequently, the interfacial adhesion between copper and the copolymer film is kept up to a certain degree in spite of the thermal degradation of the copolymer and the formation of copper oxide.

Scanning electron micrographs of the copolymer (VI/VTS = 70/30) film before and after adhesion tests are shown in *Figure 12*. *Figure 12*(*A*) hardly shows the locus where the copolymer film has flaked off the copper surface during heat treatment, but it has some cracks on the surface of the copolymer film. As shown in *Figure 12*(*B*), some copper oxide crystals exist in these cracks. The swelling of the copolymer film, beneath which copper oxide can exist, is also observed in the vicinity of the crack. *Figure 12*(*C*) shows the copper surface after adhesion test. Copper oxide is grown along the crack and the locus of interfacial failure is also observed. Its enlarged view in *Figure 12*(*D*) shows the unevenly etched copper surface and some copper oxide crystals.

For the copolymer (VI/VTS = 70/30), therefore, copper oxide formation mainly occurred in, and in the vicinity, of the crack. Considering that the interfacial adhesion strength between copper and the copolymer film is kept up after heat treatment, the copper surface beneath the copolymer film remote from the crack is thought to be, if ever, protected from corrosion. However, the possibility of a slight corrosion formation in this region cannot be excluded completely. In addition, copper oxide peaks decreased in intensities remarkably in comparison with the copolymer (VI/VTS = 85/15) (*Figure 4*). Therefore, the increase of the VTS fraction in the copolymer suppressed the diffusion of copper into the barrier film, and it also increased the thermal stability of the copolymer to prevent air oxygen from attacking copper surfaces in part.

For the copolymer (VI/VTS = 50/50), the copolymer film was not removed from copper surface after adhesion test, due to no corrosion formation at the interface and the good interfacial adhesion strength. *Figure 13* shows scanning electron micrographs of the copolymer (VI/VTS = 50/50) film heated at 360°C for 15 min in air. It shows a smooth surface and no copper oxide crystal. This suggests that the

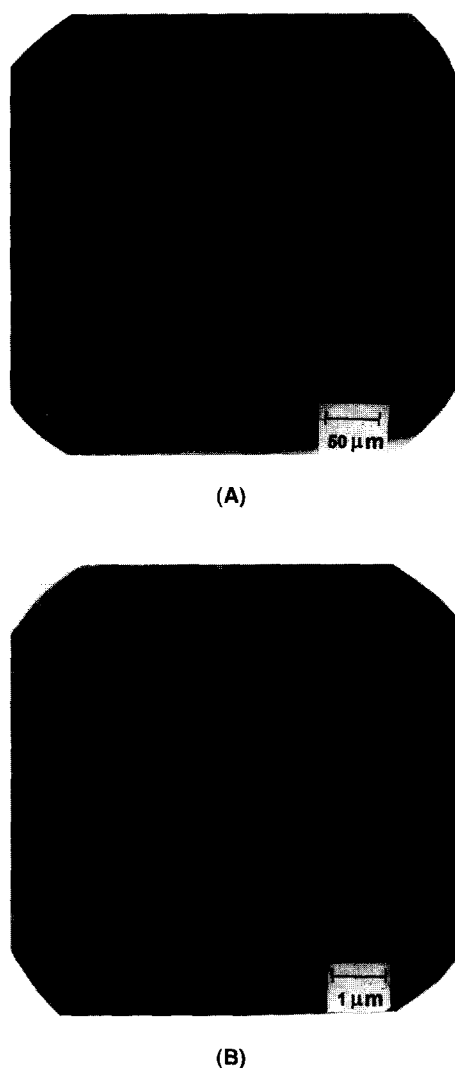

Figure 13 Scanning electron micrographs of the copolymer (VI/VTS = 50/50) film heated at 360°C for 15 min in air: (*A*) × 200 and (*B*) × 10 000

good interfacial bond at the interface is established to suppress the copper diffusion into the barrier film, and that the defect-free film with the infinite siloxane network structure is formed on copper surface.

CONCLUSIONS

Poly(VI-co-VTS)s with the different mole fractions were synthesized as a new corrosion inhibitor for copper. As shown in IR spectra and SEM photographs, copper diffusion into the bulk of the barrier film was suppressed with increasing VTS fraction in the feed.

For PVI, most of the copper oxide crystals are observed on the surface of the barrier film, due to the copper diffusion from the copper surface into the upper layer of the film by both matrix mechanism and defect mechanism. However, the introduction of VTS into PVI enhanced the thermal stability of the copolymer due to the formation of the disiloxane linkages. This improves thermal stability, reduces the formation and the size of the film defects, and suppresses copper diffusion as well as an oxygen attack into copper surface through the film defects. In addition, the VTS unit in the copolymer gives the barrier film a reactivity with copper, and the reactivity of VTS with copper contributes to the improvement of the corrosion protection capability of the copolymer. The VTS unit in the copolymer can form the Si-O-Cu bond not only with copper surface, but also with copper in the bulk of the copolymer film. Therefore, VTS unit in the copolymer can delay or inhibit the copper diffusion from surface into the bulk of the film, and also protect copper surface from the attack of air oxygen.

REFERENCES

1. Bauman, J. and Wang, J., *Inorg Chem.*, 1964, **3**, 368.
2. Chriswell, B., Lions, F. and Morris, B., *Inorg. Chem.*, 1964, **3**, 110.
3. Doonan, D. and Balch, A., *J. Am. Chem. Soc.*, 1975, **97**, 1404.
4. Salama, S. and Spiro, T. J., *Am. Chem. Soc.*, 1978, **100**, 1105.
5. Mohan, M., Bancroft, D. and Abbett, E., *Inorg. Chem.*, 1979, **18**, 1527.
6. Kolks, G., Frikart, C., Coughlin, P. and Lippard, S., *Inorg Chem.*, 1981, **20**, 2433.
7. Antolini, L., Battaglia, L., Carradi, A., Marcotrigiano, G., Menabue, L., Ellacani, G. and Saladini, M., *Inorg Chem.*, 1982, **21**, 1391.
8. Yoshida, S. and Ishida, H., *J. Chem. Phys.*, 1983, **78**, 6960.
9. Yoshida, S. and Ishida, H., *J. Mater. Sci.*, 1984, **19**, 2323.
10. Yoshida, S. and Ishida, H., *J. Adhesion*, 1984, **16**, 217.
11. Ishida, H. and Johnson, R., *Corros. Sci.*, 1986, **26**, 657.
12. Johnson, R., Daroux, M., Yeager, E. and Ishida. H., *Polymeric Materials for Corrosion Control*, ed. R. Dickie. ACS Symp. Ser. 322, American Chemical Society, Washington, DC, 1986, Ch. 23.
13. Eng, F. and Ishida, H., *J. Electrochem. Soc.*, 1988, **135**, 608.
14. Eng, F. and Ishida, H., *J. Appl. Polym. Sci.*, 1986, **32**, 5021.
15. Eng, F. and Ishida, H., *J. Appl. Polym. Sci.*, 1986, **32**, 5035.
16. Eng, F. and Ishida, H., *J. Mater. Sci.*, 1986, **21**, 1561.
17. Poling, G., *Corros. Sci.*, 1970, **10**, 359.
18. Mamsfield, F., Smith, T. and Parry, E., *Corrosion*, 1971, **27**, 289.
19. Walker, R., *Corrosion*, 1973, **29**, 290.
20. Walker, R., *Corrosion*, 1975, **31**, 97.
21. Chadwick, D. and Hashemi, T., *Corros. Sci.*, 1978, **18**, 39.
22. Fox, P., Lewis, G. and Boden, P., *Corros. Sci.*, 1979, **19**, 457.
23. Brusic, V., Frisch, M., Eldridge, B., Novak, F., Kaufman, F., Rush, B. and Frankel, G., *J. Electrochem. Soc.*, 1991, **138**, 2253.
24. Jang, J. and Ishida, H., *Corros. loci.*, 1992, **33**, 1053.
25. Jang, J. and Ishida, H. J., *Appl. Polym. Sci.*, 1993, **49**, 1957.
26. Kim, H. and Jang, J. J., *Appl. Polym. Sci.* in press.
27. Jang, J. and Kim, H. J., *Appl. Polym. Sci.*, 1995, **56**, 1495.
28. Kim, H. and Jang, J., *Polym. Bull.*, 1997, **38**, 249.
29. Bellamy, L., *The Infra-red Spectra of Complex Molecules*. Wiley, New York, 1975.
30. Colthup, N., Daly, L. and Wiberley, S., *Introduction to Infrared and Raman Spectroscopy*. Academic Press, New York, 1975.
31. Boerio, F. J. and Armogan, L., *Appl. Spectrosc.*, 1978, **32**, 509.
32. Hansen, J., Kumagai, M. and Ishida, H., *Polymer*, 1994, **35**, 4780.
33. Hansen, J. E., Rickett, B. I., Payer, J. H. and Ishida, H., *J. Polym. Sci. (B)*, 1996, **34**, 611.
34. Silverman, B. D., *Macromolecules*, 1991, **24**, 2467.
35. Legoues, F. K., Silverman, B. D. and Ho, P. S., *J. Vac. Sci. Technol. A*, 1988, **6**, 2200.
36. Faupel, F., Gupta, D., Silverman, B. D. and Ho, P. S., *Appl. Phys. Lett.*, 1989, **55**(4), 357.
37. Tromp, R. M., Legoues, F. and Ho, P. S., *J. Vac. Sci. Technol. A*, 1985, **3**, 782.
38. Burrell, M. C., Fontana, J. and Chera, J. J., *J. Vac. Sci. Technol. A*, 1988, **6**, 2893.
39. Tompkins, H. G. and Pinnel, M. R., *J. Appl. Phys.*, 1976, **47**, 3804.
40. Tompkins, H. G. and Pinnel, M. R., *J. Appl. Phys.*, 1979, **50**, 7243.